

Short-range photoassociation of LiRbD. B. Blasing,^{1,*} I. C. Stevenson,² J. Pérez-Ríos,¹ D. S. Elliott,^{1,2,3} and Y. P. Chen^{1,2,3}¹*Department of Physics and Astronomy, Purdue University, West Lafayette, Indiana 47907, USA*²*School of Electrical and Computer Engineering, Purdue University, West Lafayette, Indiana 47907, USA*³*Purdue Quantum Center, Purdue University, West Lafayette, Indiana 47907, USA*

(Received 24 August 2016; published 9 December 2016)

We have observed short-range photoassociation of ${}^7\text{Li}{}^{85}\text{Rb}$ to the two lowest vibrational states of the $d^3\Pi$ potential. We have also observed several $a^3\Sigma^+$ vibrational levels with generation rates between $\sim 10^2$ and $\sim 10^3$ molecules per second, resulting from the spontaneous decay of these $d^3\Pi$ molecules. We observe an alternation of the peak heights in the rotational photoassociation spectrum that depends on the parity of the excited molecular state. Franck-Condon overlap calculations predict that photoassociation to higher vibrational levels of the $d^3\Pi$ potential, in particular, the sixth vibrational level, should populate the lowest vibrational level of the $a^3\Sigma^+$ state at a rate as high as 10^4 molecules per second. This work also motivates an experimental search for short-range photoassociation to other bound molecular states, such as $c^3\Sigma^+$ or $b^3\Pi$, as prospects for preparing ground-state molecules.

DOI: [10.1103/PhysRevA.94.062504](https://doi.org/10.1103/PhysRevA.94.062504)**I. INTRODUCTION**

Heteronuclear bi-alkali-metal molecules in the $X^1\Sigma^+$ or $a^3\Sigma^+$ electronic potentials are interesting both experimentally and theoretically for a number of reasons. Experimentally, they have long lifetimes and large, permanent electric dipole moments. Significant effort has been dedicated to the study of dipolar molecules [1–3], in part because permanent electric dipole moments give rise to interesting long-range and anisotropic interactions [4]. For example, dipolar bosons may exhibit a pair supersolid phase [5] and enhance [6] or destabilize [7] superfluidity. They have been proposed as qubits for quantum computation [8,9], which, under certain conditions, could exhibit a high fidelity [10]. Trapped ensembles of heteronuclear bi-alkali-metal molecules could also exhibit novel few-body [11] and many-body interactions [12–14]. Such molecules could even be used to probe for variation of fundamental constants [15].

The first step in any experimental realization is, of course, the creation of the ultracold heteronuclear bi-alkali-metal molecules themselves. Two preparation methods for creating ultracold molecules stand out in particular: magnetoassociation followed by stimulated Raman adiabatic passage (STIRAP) [16] and photoassociation (PA) followed by spontaneous emission [17–23]. The PA method is experimentally simpler (as it only involves one laser), but it relies on finding an excited state that decays preferentially to the desired final state. To extend the study of the rich physics offered by ultracold heteronuclear bi-alkali-metal molecules, various preparation methods must be evaluated in a variety of systems. In this work using ultracold LiRb, we have evaluated one pathway to create $a^3\Sigma^+$ molecules, namely, PA of atoms to the $d^3\Pi$ molecular state.

Photoassociation is the process where unbound atoms, colliding in the presence of light, can absorb a photon and bind into an electronically excited-state molecule. In order to have a significant probability for this process to occur, the

matrix element between the scattering atoms and the excited molecule through the dipole operator must be large. Thus PA often occurs for excited-state molecules with large internuclear separation [24]. PA rates can also sometimes be large at short range, and heteronuclear short-range PA has been seen in LiCs [21], NaCs [22], and RbCs [23,25–28] (short-range PA has also been observed in homonuclear molecules; for some recent examples see Refs. [29] and [30]). New short-range excited-state molecules are interesting and useful to study because they can decay to deeply bound vibrational levels in the $X^1\Sigma^+$ or $a^3\Sigma^+$ electronic potentials [21–23,28,31,32]. In the present work, we report on a new short-range PA resonance to the lowest vibrational levels in the $d^3\Pi$ electronic potential of ${}^7\text{Li}{}^{85}\text{Rb}$. The $d^3\Pi$ molecules subsequently spontaneously decay to $a^3\Sigma^+$ molecules (this is similar to observations in RbCs [28]). We generate molecules bound in the $a^3\Sigma^+$ potential at a rate of $\sim 10^3$ molecules per second in the seventh lowest vibrational state. We also predict a possible extension of our work that may generate $\sim 2 \times 10^4$ molecules per second in the lowest vibrational state of the $a^3\Sigma^+$ state. A generation rate of the order of 10^4 would rank among the highest of rates for the heteronuclear bi-alkali-metal molecules in the lowest vibrational level.

II. EXPERIMENTAL APPARATUS

The details of our experimental apparatus are contained in Ref. [33], so here we provide only an overview. We work out of a dual-species LiRb MOT with a temperature of $\lesssim 1$ mK and diameter of ~ 1 mm [34]. We trap $\sim 5 \times 10^7$ Li atoms, and $\sim 1 \times 10^8$ Rb atoms, both primarily in their $F = 2$ levels. The Rb MOT is a spatial dark SPOT MOT [35]. Photoassociation of Li and Rb atoms into $d^3\Pi$ molecules is driven by an ~ 100 mW cw Ti:sapphire laser. These newly formed $d^3\Pi$ molecules then spontaneously decay, and we explore the resulting final vibrational-state distribution with resonantly enhanced multiphoton ionization (REMPI). The REMPI process is driven by a Nd:YAG-pumped, pulsed dye laser. Its frequency, ν_c , is tunable from 17 150 to 18 150 cm^{-1} when using the R590 dye, and

*dblasing@purdue.edu

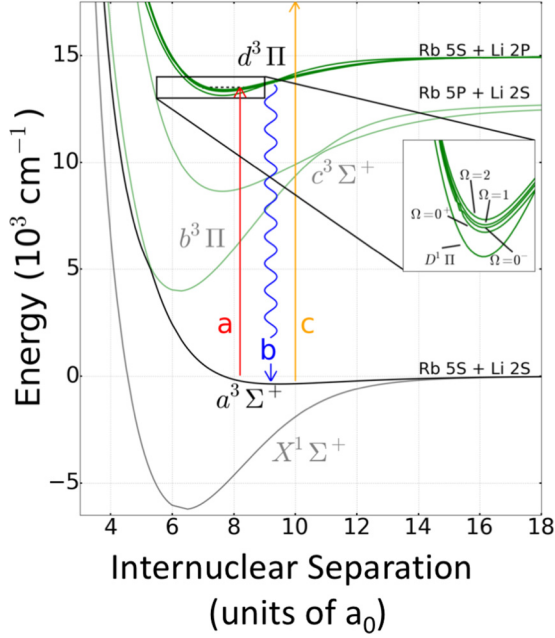


FIG. 1. Energy level diagram for the LiRb molecule showing the relevant PECs from Ref. [36]. Vertical lines show transitions, including (a) the photoassociation, with frequency ν_a ; (b) the spontaneous decay of $d^3\Pi$ molecules leading to $a^3\Sigma^+$ molecules; and (c) the first step of REMPI ionization of $a^3\Sigma^+$ molecules, at frequency ν_c , through $f^3\Pi$ (whose PEC is not shown, for clarity). The dashed horizontal black line represents our PA states. Inset: Spin-orbit components of the $d^3\Pi$ state and also the nearby $D^1\Pi$ state.

in a 4-mm-diameter beam it delivers ~ 1.5 mJ/pulse to the MOTs at a 10-Hz repetition rate. When ν_c is resonant between an initial $a^3\Sigma^+$ state and an intermediate $f^3\Pi$ state, absorption of an additional photon at frequency ν_c can ionize the molecule. Then the LiRb^+ molecular ion is accelerated with a dc electric field into a microchannel plate detector for time-of-flight-based counting. In this paper, v and J denote the vibrational and rotational levels of the $d^3\Pi_\Omega$ PA resonances, v' the vibrational states of the $f^3\Pi$ states used for REMPI, and v'' the vibrational levels of the $a^3\Sigma^+$ states which result from spontaneous decay. Ω is the projection along the internuclear axis of the total electronic angular momentum (i.e., orbital plus spin), and vibrational levels are counted up from the lowest bound state. Figure 1 shows the relevant frequencies, states, and potential energy curves (PECs).

The rest of the paper is structured as follows. In Sec. III, we discuss our PA spectroscopy to the lowest two vibrational levels of the $d^3\Pi$ state. Section IV concerns our REMPI spectroscopy of the $a^3\Sigma^+$ states that result from the spontaneous decay of one particular PA state, $d^3\Pi_{0^+}$, $v = 0$, $J = 1$. Finally, in Sec. V we offer concluding remarks and some future prospects.

III. PHOTOASSOCIATION SPECTROSCOPY OF $d^3\Pi$ STATES

We show a subset of the PA spectrum in Fig. 2, and, in Table I we list the frequencies for all the PA resonances to $d^3\Pi$ molecules that we have observed. These include the first

TABLE I. Frequencies for the observed $d^3\Pi$ PA resonances (in GHz). Uncertainties are ± 0.5 GHz, which is also the uncertainty in our wavemeter, except for $d^3\Pi_2$, $v = 0$, $J = 2$, for which it is ± 2 GHz. The additional uncertainty for the $d^3\Pi_2$, $v = 0$, $J = 2$ line position is due to its significantly lower PA strength and its more complicated structure. Blank entries denote allowed transitions that did not appear in our spectra; dashes (—) denote forbidden transitions. The $v = 0$ splittings of the spin-orbit levels are 27.3 ± 0.5 , 1074.7 ± 0.5 , and 986.4 ± 1 GHz for $\Omega = 0^+/0^-$, $1/0^+$, and $2/1$, respectively. These values differ significantly from their predicted values, which are 1080, 630, and 1140 GHz, respectively [36]. (Our group also found disagreement between experiment and theory for the spin-orbit splittings in the past of the $f^3\Pi$ state [34]. Further, a small spin-orbit splitting between $\Omega = 0^-$ and 0^+ was observed in KRb [37].) The J -dependent parity for $\Omega \neq 0$ states was not resolved since the Δ doubling is small for the low-lying rotational states accessed. The spin-orbit splittings and rotational constants (B_v) agree with our recent depletion spectroscopy [32].

v	Ω	$J = 0$	$J = 1$	$J = 2$	$J = 3$	B_v
0	0^-	404 952.0	404 961.0	404 978.5	405 006.8	4.5
0	0^+		404 988.1	405 005.9		4.5
0	1	—	406 062.7	406 080.6	406 108.4	4.5
0	2	—	—	407 067		
1	0^-	407 918.6	^a	407 944.9		4.4
1	0^+		407 952.0			
1	1	—	409 037.4	409 054.9		4.4

^aWe observed a peak in the PA spectrum at 407 928.2 GHz, which is 800 MHz higher than the predicted value of 407 927.4 GHz using the rotational constant of 4.4 GHz (as determined by the other peaks in the series). The identity of this peak is unclear since 800 MHz is also our Li hyperfine spacing.

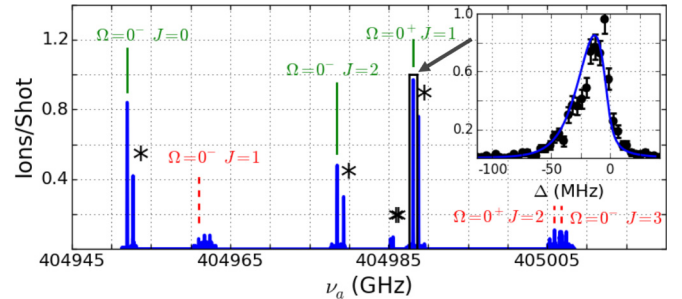


FIG. 2. PA spectrum of the $d^3\Pi$, $v = 0$ state. We observe PA to molecules with $J = 0$ to 3 and have labeled PA to molecules with positive and negative parity as dashed red lines and solid green lines, respectively. This parity alternates based on the J quantum number in the $\Omega = 0^\pm$ states. These assignments are consistent with those determined by depletion spectroscopy to the same states [32]. Our assignments indicate that free-to-bound PA transitions to molecular states with negative parity are significantly stronger than their positive-parity counterparts, sometimes by almost an order of magnitude. For these scans, the REMPI laser was tuned to the transition from $a^3\Sigma^+$, $v'' = 7$ to $f^3\Pi_0$, $v' = 4$ at $17\,654.8$ cm^{-1} . Inset: High-resolution PA scan to the $\Omega = 0^+$, $J = 1$ state with a fit based on Eq. (1). Δ is the detuning from the fitted peak center. An asterisk denotes a hyperfine echo from the MOT population in Li $F = 1$ or Rb $F = 3$ atoms.

and second vibrational levels and their four spin-orbit split states: $\Omega = 0^+, 0^-, 1$, and 2 . (The assignments of $\Omega = 0^+$ and $\Omega = 0^-$ have some ambiguity, which is discussed later in this section.) The most interesting feature in Fig. 2 is the strong alternation of the PA rate with the J quantum number within each $\Omega = 0^\pm$ progression. Within each $\Omega = 0^\pm$ progression, the solid green and dashed red labels for increasing J refer to the parity of the total molecular wave function of the PA state upon coordinate inversion through the origin in the laboratory frame [38]. (This is not to be confused with the \pm label for the $\Omega = 0^\pm$ states, which refers to the parity of the total molecular wave function upon reflecting just the electronic coordinates through a plane containing both nuclei.) For $\Omega = 0^+$, the parity is $(-1)^J$, while for $\Omega = 0^-$, it is $(-1)^{J+1}$.

Enhancement and suppression of different rotational lines in PA spectra have been observed before, in both homonuclear and heteronuclear molecules [21,39,40]. (For alternate examples where such an effect was not observed, see Refs. [26–28] and [41].) The presence or absence of individual rotational lines can be affected by many factors, for example, the spins of the colliding atoms [42] or a scattering resonance that enhances the contribution of a particular partial wave, which has a well-defined parity, to the PA signal. Of course, since for dipole transitions, the parity of the initial and final states must be opposite, observing such a parity-dependent PA rate in LiRb seemingly requires our initial and final states to have reasonably well-defined, opposite parities. Therefore, a possible explanation of our higher PA rates to states with a negative parity is that, at the temperature of our MOTs, a partial wave with positive parity makes the largest contribution to the collision cross section between Li and Rb. The parity of the ℓ th partial wave is $(-1)^\ell$, where ℓ is the quantum number for the angular momentum of the collision; the lowest partial wave with a positive parity is the $\ell = 0$ (s wave).

Several aspects of our data support our interpretation that the scattering state has significant s -wave nature at the temperature of our MOTs. First, in the present work, we observe a PA rate that alternates for J states of the $\Omega = 0^\pm$, but not for $J = 1$ and 2 of the $\Omega = 1$. For $\Omega = 0^\pm$, different J states alternate in parity, but for $\Omega = 1$, two bound states, one with positive-parity and one with negative-parity, are degenerate for each J state [38]. Also, since PA to $J = 3$ was only weakly observable for one $\Omega = 0$ series and not for the other and, further, the p wave but not the s wave can access $J = 3$ through PA, the most significant wave of the scattering state is most likely the s wave and not the p wave. (We also found that PA to $J = 3$ of $\Omega = 1$, for which both parities are available, was also weak.) In Fig. 3 we show our interpretation of the different partial waves responsible for the PA spectrum in Fig. 2, with s -wave contributions shown as solid green lines and p -wave contributions as dashed red lines. Second, in another, separate PA experiment, we were able to infer PA to odd-parity states of other electronic states [32]. The final argument in favor of s -wave scattering, as discussed further below, is that at the temperature of our MOTs, calculations of the elastic scattering cross section show that the s wave contributes significantly more than the p wave.

The temperature, T , of the collisions between Li and Rb in our MOTs was extracted by fitting the experimental line shape

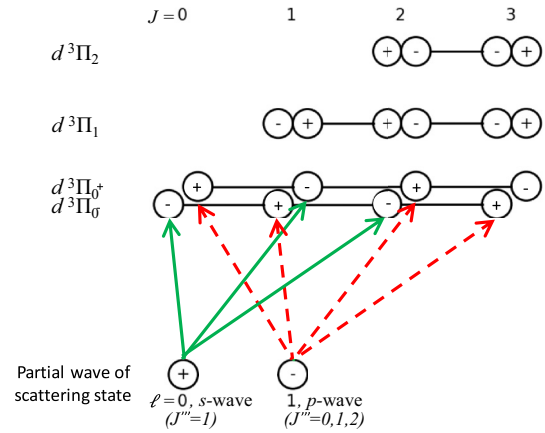


FIG. 3. Parities for the partial waves of the scattering state and final $d^3\Pi_\Omega$ states, adapted and modified from Ref. [38]. Solid green and dashed red arrows correspond, respectively, to the alternating strong- and weak-dipole-allowed PA transitions to the $d^3\Pi_0$ state shown in Fig. 2. The parity of every state or wave is shown as a circled plus or minus sign. Transitions to $\Omega = 1$ or 2 states and the small energy splitting of the J states are not shown, for clarity. Note that we can resolve the energy splitting between different parities for $\Omega = 0^\pm$ states but not for $\Omega = 1$ or 2 states. J'' refers here to the total angular momentum of the scattering state along the $a^3\Sigma^+$ potential for scattering through different partial waves.

of the PA resonances with a convolution of a Boltzmann with a Lorentzian [43], which is valid for temperatures below the van der Waals energy of ~ 1 mK,

$$W(f, f_0) \propto \sum_l \int_0^\infty e^{-\frac{h\nu}{k_B T}} v^{\ell+\frac{1}{2}} L_\Gamma(f, f_0 - \nu) d\nu, \quad (1)$$

where $L_\Gamma(f, f_0)$ stands for a Lorentzian function with central frequency f_0 and natural line width Γ , and k_B and h denote the Boltzmann and Planck constants, respectively. We fit our PA resonances with Eq. (1) using four free parameters: the overall amplitude, the natural line width Γ , the resonant frequency f_0 , and the collision temperature T . For example, the inset in Fig. 2 shows the PA spectrum for the $J = 1$ level of the $\Omega = 0^+$ electronic state and its fit. The fit assuming s -wave scattering yielded $T = 440 \pm 70 \mu\text{K}$ and $\Gamma/2\pi = 9 \pm 2$ MHz. (The data can also be fit with $\ell = l$, p -wave scattering, yielding similar temperatures and a comparable fit quality measured by R^2 values. Additionally, it is also possible to fit PA spectra with several partial waves. For these reasons, ℓ for the scattering state cannot be determined from the fits alone.)

With the extracted temperature of $440 \mu\text{K}$, we then used many of the currently available PECs for LiRb [36,44,45] to calculate the contributions to the elastic scattering cross section of the few lowest partial waves at various temperatures including $440 \mu\text{K}$. The calculations predicted that the s -wave contribution is approximately one order of magnitude larger than that of the p -wave. However, we do note that such calculations depend very sensitively on the PEC. (Our calculations using the PECs cited above were sufficient to derive the binding energies of most of the vibrational levels reasonably well and a scattering length consistent with those previously predicted [46,47]. We did not exhaust the

PECs available in the literature; for further examples, see Refs. [48–50].) The above reasons support our conclusion that the s wave is likely the dominant partial wave for the colliding Li and Rb atoms in this experiment. We also note that our scattering state mostly consists of just a single partial wave, which leads to both the oscillation of the PA rate in the $\Omega = 0$ series and the sharp cutoff at $J = 2$.

It should be noted that our assignment of $\Omega = 0^-$ as being lower in energy than $\Omega = 0^+$ is not without some hesitancy. The first reason is that our assignment disagrees with the predicted ordering [36], which is shown in Fig. 1. The resolution of this disagreement between the interpretation of our experimental work and the theoretical calculations remains to be understood. (Adopting the predicted ordering would bring difficulty in interpreting our current data. Such an ordering would flip the parity of every state in the two $\Omega = 0$ series, and then explaining the $\Omega = 0$ states with strong PA would require a p -wave shape resonance. Such a shape resonance is unsupported by the PECs we used. Further, it would be inconsistent with our observation of weak PA to $J = 3$.) We also noted the difficulty of assigning $\Omega = 0^-$ and $\Omega = 0^+$ with certainty in previous experiments on RbCs [23,25–28]. That said, our assignments of $\Omega = 0^-$ and $\Omega = 0^+$ are made with some confidence but not with total certainty.

IV. REMPI SPECTROSCOPY OF $a^3\Sigma^+$ STATES

After exploring the properties of the PA to the $d^3\Pi$, we investigated the spontaneous decay of the $d^3\Pi_{0^+}$, $v = 0$, $J = 1$ state with REMPI spectroscopy. For this spectroscopy we locked the Ti:Sapphire laser to the PA resonance of the $d^3\Pi_{0^+}$, $v = 0$, $J = 1$ state. The motivation for this was to explore deeply bound molecules of the $a^3\Sigma^+$ potential, perhaps even its lowest vibrational level. We show a sample REMPI spectrum, with transitions from $a^3\Sigma^+$, $v'' = 2, 4, 6$, and 7 in Fig. 4. In previous studies, we have used PA (to other bound states) followed by REMPI spectroscopy to detect $a^3\Sigma^+$, $v'' = 7$ through 13 [34]. In the current study, and from the whole REMPI spectrum, the progressions for $v'' = 2, 4, 6, 7, 8, 9$, and 10 are reasonably clear. However, ionizing $a^3\Sigma^+$

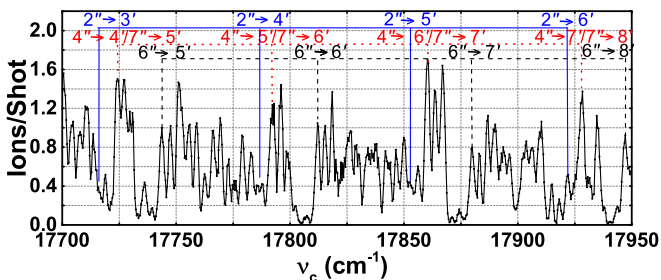


FIG. 4. Sample REMPI spectrum. Solid blue, dotted red, and dashed black lines, respectively, are our assignments for progressions from $a^3\Sigma^+$, $v'' = 2$, some combination of $v'' = 4$ or 7, and $v'' = 6$ to vibrational levels $v' = 3-8$ of the $f^3\Pi_0$ state. Each data point is the average of 100 REMPI pulses and is smoothed by averaging over nearest neighbors. (Although not labeled here, we have assignments for more than 90% of the observed REMPI resonances.)

TABLE II. Binding energies (E_B) of $a^3\Sigma^+$ v'' states extracted from our REMPI spectrum. The binding energies for $v'' = 2, 5, 6, 7, 8, 9$, and 10 have uncertainties of $\pm 0.2 \text{ cm}^{-1}$. The binding energies for $v'' = 1$ and 4 have uncertainties of $\pm 1 \text{ cm}^{-1}$ since their REMPI lines occurred in regions with significant line congestion. Blank entries correspond to states and binding energies which we were not able to determine from the REMPI spectrum. The theoretical predictions use the potential energy curves from Refs. [36] and [44] with the LEVEL 8.0 code [51].

$a^3\Sigma^+v''$	$E_B \text{ (cm}^{-1}\text{)}$		$E_B(v'') - E_B(v'' + 1) \text{ (cm}^{-1}\text{)}$	
	Expt.	Theor.	Expt.	Theor.
0		257.7		37.7
1	222	220.0	35	34.6
2	186.7	185.4		31.7
3		153.7		28.7
4	126	125.0	26	25.7
5	99.8	99.3	23.0	22.7
6	76.8	76.5	19.6	19.8
7	57.2	56.8	16.6	16.7
8	40.6	40.1	13.9	13.6
9	26.7	26.5	10.2	10.4
10	16.5	16.1		7.4
13	1.08 ^a	1.1		1.0

^aThis value was extracted from depletion spectroscopy using a different PA resonance [32] in combination with the PA data presented here and has an uncertainty of 0.02 cm^{-1} ; the higher precision of this binding energy allowed us to extract the other binding energies at the level of ~ 0.1 to 1 cm^{-1} .

states $v'' = 1$ and 4 through the $f^3\Pi$ states results in congested REMPI peaks and our assignments are less certain.

From the REMPI spectrum and our previous spectroscopy of the $f^3\Pi_0$ states [34], we extracted binding energies for some new, lower vibrational levels of the $a^3\Sigma^+$ states as listed in Table II. Further experiments, particularly depletion spectroscopy, would refine our line assignments and binding energies. Our REMPI spectrum did not conclusively reveal the $v'' = 0$ state of the $a^3\Sigma^+$ potential. Unfortunately, other stronger REMPI lines obscured any weak lines that may have originated from $v'' = 0$ molecules.

V. CONCLUSIONS AND FUTURE PROSPECTS

For many future uses of polar molecules, the rate, R , of generating molecules is important. To estimate R , we follow the standard procedure, similar to that used in Refs. [21,28,31,52]. For the strongest and weakest REMPI lines we measured, assigned to $a^3\Sigma^+$, $v'' = 7$ and $v'' = 2$, we find rates of $\approx 2.5 \times 10^3$ molecules and $\approx 4 \times 10^2$ per second, respectively. The generation rates of the other vibrational levels of the $a^3\Sigma^+$ should fall between those values. We are currently building a 1064-nm optical dipole trap to confine both Li and Rb. This will increase the densities of both species and reduce both their temperatures, thus leading to a higher PA rate.

Future experiments may need large amounts of $a^3\Sigma^+$, $v'' = 0$ molecules in particular. To offer somewhat reasoned speculation about generating such molecules, we estimated the

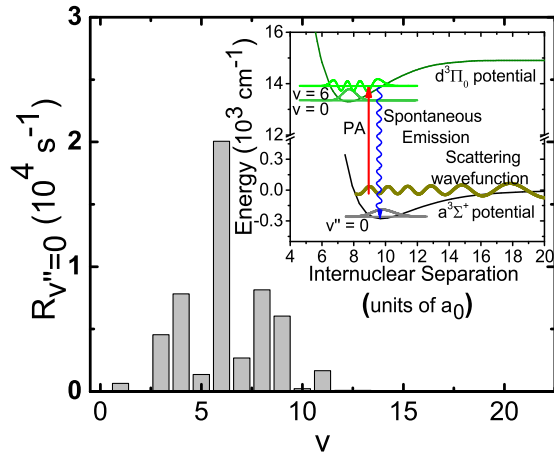


FIG. 5. Predicted generation rates, R , of the $a^3\Sigma^+$, $v'' = 0$ state using PA to different vibrational levels v of the $d^3\Pi$ states. To generate this plot, we assumed experimental conditions similar to those we used in the present work except, of course, for the frequency of the PA laser. Inset: Sketch of PECs, bound wave functions of interest, and the scattering wave function at $500 \mu\text{K}$. Note the high generation rate of $v'' = 0$ predicted from PA using the $d^3\Pi$, $v = 6$ state.

free-to-bound overlaps for hypothetical PA steps to various v values of the $d^3\Pi$ state using the Numerov method and the Franck-Condon factors (FCFs) for the spontaneous emission step down to $v'' = 0$ of the $a^3\Sigma^+$ state using LEVEL 8.0. As validations of such methods, the Numerov calculations predicted roughly comparable PA rates to $v = 0$ and 1 of the $d^3\Pi$ state, which was confirmed, and the FCF calculations qualitatively predicted the distribution of v'' of the $a^3\Sigma^+$ state that we measured in our REMPI spectrum. Further, in the past, we found FCFs to have semiquantitative predictive value for bound-to-bound transitions [34,53].

Our calculations revealed that PA to the $v = 6$ of the $d^3\Pi$ state may generate $v'' = 0$ molecules at significant rates, even

when compared to our largest measured REMPI line, which is assigned to $v'' = 7$. (Our Ti:sapphire laser cannot produce frequencies for PA to levels higher than $v = 1$.) In Fig. 5, we plot the predicted $R_{v''=0}$ for PA to various vibrational states of the $d^3\Pi$ state, assuming experimental conditions similar to those used in this present work. We find that, if we had been able to PA to $v = 6$ of the $d^3\Pi$ state, it may have produced $a^3\Sigma^+$, $v'' = 0$ molecules at approximately seven times the rate of our measured generation of $v'' = 7$ molecules. Further, the insignificant $R_{v''=0}$ with PA to $v = 0$ is consistent with our REMPI scan; we were unable to identify a clear series of REMPI peaks from $v'' = 0$, but we easily identified a large series of peaks for $v'' = 7$. Therefore, studying the REMPI spectrum that instead results from spontaneous decay from PA to $v = 6$ of the $d^3\Pi$ state may result in $R_{v''=0}$ as high as $\sim 2 \times 10^4$ molecules per second and, also, fix the $a^3\Sigma^+$ well depth.

Our experiments open a number of avenues for further work. Our PA spectrum seemingly indicates that $\Omega = 0^-$ is lower in energy compared to $\Omega = 0^+$, which is inconsistent with previous calculations. Resolving this apparent contradiction may involve further experimental and theoretical work. Our work also motivates a search for short-range PA to the $c^3\Sigma^+$ state and the $b^3\Pi$ state, perhaps finding an excited state that decays preferentially to a small number of vibrational levels in the $a^3\Sigma^+$ potential; the $v = 6$ state of the $d^3\Pi$ state may provide such preferential decay and form $a^3\Sigma^+$, $v'' = 0$ molecules at significant rates. As such, our experiment lays a solid groundwork towards efficient preparation of triplet molecular samples and the further experiments that need them.

ACKNOWLEDGMENTS

We acknowledge helpful discussions with and the work of Sourav Dutta, Adeel Altaf, and John Lorenz. The experimental work was funded by the Purdue Office of the Vice President for Research AMO Incentive Grant 206732 and J.P.-R. acknowledges support from NSF Grant No. PHY-130690.

The first two authors contributed equally to this article.

- [1] M. A. Baranov, *Phys. Rep.* **464**, 71 (2008).
- [2] R. V. Krems, W. C. Stwalley, and B. Friedrich (eds.), *Cold Molecules: Theory, Experiment, Applications* (CRC Press, Boca Raton, FL, 2009).
- [3] T. Lahaye, C. Menotti, L. Santos, M. Lewenstein, and T. Pfau, *Rep. Prog. Phys.* **72**, 126401 (2009).
- [4] K.-K. Ni, S. Ospelkaus, D. Wang, G. Quémener, B. Neyenhuis, M. H. G. de Miranda, J. L. Bohn, J. Ye, and D. S. Jin, *Nature* **464**, 1324 (2010).
- [5] C. Trefzger, C. Menotti, and M. Lewenstein, *Phys. Rev. Lett.* **103**, 035304 (2009).
- [6] A. V. Gorshkov, S. R. Manmana, G. Chen, J. Ye, E. Demler, M. D. Lukin, and A. M. Rey, *Phys. Rev. Lett.* **107**, 115301 (2011).
- [7] C. Zhang, A. Safavi-Naini, A. M. Rey, and B. Capogrosso-Sansone, *New J. Phys.* **17**, 123014 (2015).
- [8] D. DeMille, *Phys. Rev. Lett.* **88**, 067901 (2002).
- [9] S. F. Yelin, K. Kirby, and R. Côté, *Phys. Rev. A* **74**, 050301 (2006).
- [10] P. Rabl and P. Zoller, *Phys. Rev. A* **76**, 042308 (2007).
- [11] H. P. Büchler, A. Micheli, and P. Zoller, *Nature Phys.* **3**, 726 (2007).
- [12] J. Pérez-Ríos, F. Herrera, and R. V. Krems, *New J. Phys.* **12**, 103007 (2010).
- [13] D.-W. Wang, M. D. Lukin, and E. Demler, *Phys. Rev. Lett.* **97**, 180413 (2006).
- [14] A. Micheli, G. K. Brennen, and P. Zoller, *Nature Phys.* **2**, 341 (2006).
- [15] C. Chin, V. V. Flambaum, and M. G. Kozlov, *New J. Phys.* **11**, 055048 (2009).
- [16] K.-K. Ni, S. Ospelkaus, M. H. G. de Miranda, A. Pe'er, B. Neyenhuis, J. J. Zirbel, S. Kotochigova, P. S. Julienne, D. S. Jin, and J. Ye, *Science* **322**, 231 (2008).

- [17] A. Fioretti, D. Comparat, A. Crubellier, O. Dulieu, F. Masnou-Seeuws, and P. Pillet, *Phys. Rev. Lett.* **80**, 4402 (1998).
- [18] T. Takekoshi, B. M. Patterson, and R. J. Knize, *Phys. Rev. A* **59**, R5 (1999).
- [19] A. N. Nikolov, E. E. Eyler, X. T. Wang, J. Li, H. Wang, W. C. Stwalley, and P. L. Gould, *Phys. Rev. Lett.* **82**, 703 (1999).
- [20] A. J. Kerman, J. M. Sage, S. Sainis, T. Bergeman, and D. DeMille, *Phys. Rev. Lett.* **92**, 153001 (2004).
- [21] J. Deiglmayr, A. Grochola, M. Repp, K. Mörtlbauer, C. Glück, J. Lange, O. Dulieu, R. Wester, and M. Weidemüller, *Phys. Rev. Lett.* **101**, 133004 (2008).
- [22] P. Zabawa, A. Wakim, M. Haruza, and N. P. Bigelow, *Phys. Rev. A* **84**, 061401(R) (2011).
- [23] A. Fioretti and C. Gabbanini, *Phys. Rev. A* **87**, 054701 (2013).
- [24] K. Jones, E. Tiesinga, P. Lett, and P. Julienne, *Rev. Mod. Phys.* **78**, 483 (2006).
- [25] C. Gabbanini and O. Dulieu, *Phys. Chem. Chem. Phys.* **13**, 18905 (2011).
- [26] Z. Ji, H. Zhang, J. Wu, J. Yuan, Y. Yang, Y. Zhao, J. Ma, L. Wang, L. Xiao, and S. Jia, *Phys. Rev. A* **85**, 013401 (2012).
- [27] N. Bouloufa-Maafa, M. Aymar, O. Dulieu, and C. Gabbanini, *Laser Phys.* **22**, 1502 (2012).
- [28] C. D. Bruzewicz, M. Gustavsson, T. Shimasaki, and D. Demille, *New J. Phys.* **16**, 023018 (2014).
- [29] C. R. Menegatti, B. S. Marangoni, N. Bouloufa-Maafa, O. Dulieu, and L. G. Marcassa, *Phys. Rev. A* **87**, 053404 (2013).
- [30] R. A. Carollo, J. L. Carini, E. E. Eyler, P. L. Gould, and W. C. Stwalley, *J. Phys. B: At. Mol. Opt. Phys.* **49**, 194001 (2016).
- [31] J. Banerjee, D. Rahmlow, R. Carollo, M. Bellos, E. E. Eyler, P. L. Gould, and W. C. Stwalley, *Phys. Rev. A* **86**, 053428 (2012).
- [32] I. Stevenson, D. Blasing, A. Altaaf, Y. P. Chen, and D. S. Elliott, *J. Chem. Phys.* (2016) (to be published).
- [33] S. Dutta, A. Altaf, J. Lorenz, D. S. Elliott, and Y. P. Chen, *J. Phys. B* **47**, 105301 (2014).
- [34] A. Altaf, S. Dutta, J. Lorenz, J. Pérez-Ríos, Y. P. Chen, and D. S. Elliott, *J. Chem. Phys.* **142**, 114310 (2015).
- [35] W. Ketterle, K. B. Davis, M. A. Joffe, A. Martin, and D. E. Pritchard, *Phys. Rev. Lett.* **70**, 2253 (1993).
- [36] M. Korek, G. Younes, and S. AL-Shawa, *J. Mol. Struct. (THEOCHEM)* **899**, 25 (2009).
- [37] J. Banerjee, D. Rahmlow, R. Carollo, M. Bellos, E. E. Eyler, P. L. Gould, and W. C. Stwalley, *J. Chem. Phys.* **138**, 164302 (2013).
- [38] G. Herzberg, *Molecular Spectra and Molecular Structure. I. Spectra of Diatomic Molecules*, 2nd ed. (Krieger, Malabar, FL, 1989).
- [39] H. M. J. M. Boesten, C. C. Tsai, J. R. Gardner, D. J. Heinzen, and B. J. Verhaar, *Phys. Rev. A* **55**, 636 (1997).
- [40] M. A. Bellos, R. Carollo, D. Rahmlow, J. Banerjee, E. E. Eyler, P. L. Gould, and W. C. Stwalley, *Phys. Rev. A* **86**, 033407 (2012).
- [41] M. A. Bellos, D. Rahmlow, R. Carollo, J. Banerjee, O. Dulieu, A. Gerdes, E. E. Eyler, P. L. Gould, and W. C. Stwalley, *Phys. Chem. Chem. Phys.* **13**, 18880 (2011).
- [42] J. R. Gardner, R. A. Cline, J. D. Miller, D. J. Heinzen, H. M. J. M. Boesten, and B. J. Verhaar, *Phys. Rev. Lett.* **74**, 3764 (1995).
- [43] K. M. Jones, P. D. Lett, E. Tiesinga, and P. S. Julienne, *Phys. Rev. A* **61**, 012501 (1999).
- [44] M. Ivanova, A. Stein, A. Pashov, H. Knöckel, and E. Tiemann, *J. Chem. Phys.* **134**, 024321 (2011).
- [45] R. A. W. Maier, M. Eisele, E. Tiemann, and C. Zimmermann, *Phys. Rev. Lett.* **115**, 043201 (2015).
- [46] C. Marzok, B. Deh, C. Zimmermann, P. W. Courteille, E. Tiemann, Y. V. Vanne, and A. Saenz, *Phys. Rev. A* **79**, 012717 (2009).
- [47] J. Pérez-Ríos, S. Dutta, Y. P. Chen, and C. H. Greene, *New J. Phys.* **17**, 045021 (2015).
- [48] R. Dardouri, H. Habli, B. Oujia, and F. X. Gadéa, *J. Comput. Chem.* **34**, 2091 (2013).
- [49] Y. You, C.-L. Yang, M.-S. Wang, X.-G. Ma, W.-W. Liu, and L.-Z. Wang, *Spectrochim. Acta A: Mol. Biomol. Spectrosc.* **153**, 488 (2016).
- [50] Y. You, C.-L. Yang, Q.-Q. Zhang, M.-S. Wang, X.-G. Ma, and W.-W. Liu, *Phys. Chem. Chem. Phys.* **18**, 19838 (2016).
- [51] R. J. L. Roy, *J. Quant. Spectrosc. Radiat. Transfer* **186**, 167 (2017).
- [52] I. Stevenson, D. Blasing, Y. P. Chen, and D. S. Elliott, [arXiv:1603.02567v3](https://arxiv.org/abs/1603.02567v3) [*Phys. Rev. A* (to be published)].
- [53] J. Lorenz, A. Altaf, S. Dutta, Y. P. Chen, and D. S. Elliott, *Phys. Rev. A* **90**, 062513 (2014).